On Physical Layer Security Over Generalized Gamma Fading Channels

Hongjiang Lei, Chao Gao, Yongcai Guo, and Gaofeng Pan, *Member, IEEE*

***Abstract*—In this letter, we study the secrecy performance of the classic Wyner's wiretap model over the generalized Gamma fading channels. The closed-form expressions for the probability of strictly positive secrecy capacity and the lower bound of secure outage probability are derived. Monte-Carlo simulations are performed to verify the derived analysis.**

***Index Terms*—Physical layer security, generalized gamma channel, secure outage probability.**

I. INTRODUCTION

RECENTLY, there was an ever increasing interest of exploring the secrecy performance in digital communications over fading channels. The probability of strictly positive secrecy capacity (SPSC) was studied for the systems over independent log-normal fading channel with single eavesdropper and multiple eavesdroppers in [1], [2], respectively. A closed-form expression for SPSC over the Rician and Weibull fading channels were drived in [3], [4], respectively. The secrecy outage probability (SOP) over correlated log-normal fading channels was investigated in [5]. Sun etc. derived infinite-series representations for both the average secrecy capacity and the SOP of secure communications over correlated Rayleigh fading wiretap channels [6]. Ref. [7] presented several diversity techniques for improving wireless security against eavesdropping attacks. Several optimal relay selection schemes were proposed to improve the physical-layer security in wireless cooperative networks and cognitive radio network in [8] and [9], respectively.

The generalized Gamma (GG) distribution, which was first proposed by Stacy [10], was purely a mathematical problem in which some statistical properties of a generalized version of the Gamma distribution were investigated. Yacoub rewrote the form of the GG distribution as the α-μ distribution [11], [12], in which the parameters are directly associated with the physical properties of the propagation medium. The GG or α-μ distribution is general, flexible, and has easy mathematical tractability. It includes important distributions such as Gamma, Nakagami-m, exponential, Weibull, and Rayleigh. Its density, cumulative frequency, and moments appear in simple closed form expressions. All these features combined make the GG or α-μ distribution very attractive.

So far, most of the references about the physical layer security focus their concentration either on small-scale fading channels (i.e., Rayleigh, Rice, Nakagami-m) or on large-scale fading channels (i.e., log-normal fading channels) [1]–[6], [13]. All these works just propose analytical models for a particular type of fading channels and cannot cover various fading types in practical scenarios. It is well known that GG fading distribution is more general and flexible as it includes some important distributions, such as Gamma, Nakagami-m, exponential, Weibull, and Rayleigh. On the other hand, the existing works on GG fading channels are limited to analyzing common end-to-end communication performance, such as outage probability [14], average bit error probability [15], and ergodic capacity [16]. To the best of the authors' knowledge, there has been no previous published works related to the physical layer security over GG fading channels, especially on the classic Wyner's model [17].

Motivated by this observation, in this work we propose analytical models on SOP and SPSC to study the physical layer security, which can be easily applied in more common fading scenarios.

II. SYSTEM MODEL

In this letter, the classic Wyner's wiretap model [17] is considered, where the source S sends confidential messages to the legitimate receiver D over the main channel while the eavesdropper E attempts to decode these messages from its received signal through the eavesdropper channel. It is assumed that the main and eavesdropper channels experience independent GG fading, and suffer from independent complex Gaussian noises with zero-mean and unit-variances. Both channels experience the ergodic block fading where channel coefficients remain constants during a block period, vary independently across blocks. Furthermore, we also assume that the full channel state information of both the main and eavesdropper channels is available at S.

The GG distribution is given by [14]–[16], [18] as

$$f_R(r) = \frac{\alpha c^c r^{\alpha c-1}}{\Gamma(c)\bar{r}^{\alpha c}} \exp\left(-c\left(\frac{r}{\bar{r}}\right)^{\alpha}\right), \alpha > 0, c > 0, \quad (1)$$

where $\Gamma(c) = \int_0^\infty t^{c-1}e^{-t}dt$ is the well-known Gamma function, α is a fading parameter, c is the normalized variance of the channel envelope R, and $\bar{r}$ is the α-root mean value of the channel envelope. This distribution is a general form for many well-known distributions such as Rayleigh ($\alpha = 2,\ c = 1$), Nakagami-m ($\alpha = 2$, and c is the fading parameter), Weibull ($c = 1$, and α is the fading parameter).

Manuscript received February 11, 2015; accepted April 21, 2015. Date of publication April 24, 2015; date of current version July 8, 2015. The work is supported in part by the National Natural Science Foundation of China (NSFC) under Grant no. 61379159, 61401372, Natural Science Foundation Project of CQ CSTC under Grant no. cstc2011jjA40043, cstc2012jjA40040, 2013jcyjA40040, Research Fund for the Doctoral Program of Higher Education of China under Grant no. 20130182120017. The associate editor coordinating the review of this paper and approving it for publication was Y. Zou.

H. Lei is with the Key Laboratory of Optoelectronics Technology and System, Ministry of Education, Chongqing University, Chongqing 400044, China, and also with Chongqing Key Lab of Mobile Communications Technology, Chongqing University of Posts and Communications, Chongqing 400065, China. (e-mail: leihj@cqupt.edu.cn).

C. Gao and Y. Guo are with the Key Laboratory of Optoelectronic Technology and Systems of the Education Ministry of China, Chongqing University, Chongqing 400044, China. (e-mail: gaoc@cqu.edu.cn; ycguo@cqu.edu.cn).

G. Pan is with the School of Electronic and Information Engineering, Southwest University, Chongqing, 400715, China (e-mail: gfpan@swu.edu.cn).

Digital Object Identifier 10.1109/LCOMM.2015.2426171

The probability density function (PDF) and cumulative distribution function (CDF) of signal-to-noise ratio (SNR) for GG fading channel is given by [16] as

$$f_k(\gamma)=\frac{\alpha_k c_k^{c_k}\gamma^{\frac{\alpha_k c_k}{2}-1}}{2(\bar{\gamma}_k)^{\frac{\alpha_k c_k}{2}}\Gamma(c_k)}\exp\left(-c_k\left(\frac{\gamma}{\bar{\gamma}_k}\right)^{\frac{\alpha_k}{2}}\right), k\in\{D,E\}, \tag{2}$$

and

$$F_k(\gamma)=\frac{\Upsilon\left(c_k, c_k\left(\frac{\gamma}{\bar{\gamma}_k}\right)^{\frac{\alpha_k}{2}}\right)}{\Gamma(c_k)}, k\in\{D,E\}, \tag{3}$$

respectively, where $\alpha_k(k\in\{D,E\})$ is the fading parameters of the main and eavesdropper channels, respectively. $c_k(k\in\{D,E\})$ is the normalized variances of the main and eavesdropper channel envelopes, respectively. $\bar{\gamma}_k=E[{R_k}^2]\frac{E_b}{N_0}(k\in\{D,E\})$ is the average SNR at D and E, respectively, $\frac{E_b}{N_0}$ is the energy per bit to the noise power spectral density ratio. $\Upsilon(\alpha,x)=\int_0^x e^{-t}t^{\alpha-1}dt$ is the lower incomplete Gamma function, as defined by Eq. (8.350/1) in [19].

III. SOP Analysis

SOP, which is defined in [20] as the probability that the instantaneous secrecy capacity falls below a target rate, is an important performance measure and widely used to characterize wireless communications. SOP can be presented as

$$\begin{aligned}
SOP &= P\left\{C_s(\gamma_D,\gamma_E)\le C_{th}\right\}\\
&= P\left\{\ln(1+\gamma_D)-\ln(1+\gamma_E)\le C_{th}\right\}\\
&= P\{\gamma_D\le\Theta\gamma_E+\Theta-1\}\\
&= \int_0^\infty\int_0^{\Theta\gamma_E+\Theta-1} f_D(\gamma_D)d\gamma_D f_E(\gamma_E)d\gamma_E\\
&= \int_0^\infty F_D(\Theta\gamma_E+\Theta-1)f_E(\gamma_E)d\gamma_E\\
&= \frac{\alpha_E}{2\beta_E^{c_E}\Gamma(c_D)\Gamma(c_E)}\left(\int_0^\infty \gamma_E^{\frac{\alpha_E c_E}{2}-1}\exp\left(-\frac{\gamma_E^{\frac{\alpha_E}{2}}}{\beta_E}\right)\right.\\
&\quad \left.\times\Upsilon\left(c_D,\frac{(\Theta\gamma_E+\Theta-1)^{\frac{\alpha_D}{2}}}{\beta_D}\right)d\gamma_E\right)\\
&= \frac{\alpha_E}{2\beta_E^{c_E}\Gamma(c_D)\Gamma(c_E)}\left(\int_0^\infty \gamma_E^{\frac{\alpha_E c_E}{2}}-1\exp\left(-\frac{\gamma_E^{\frac{\alpha_E}{2}}}{\beta_E}\right)\right.\\
&\quad \left.\times\Upsilon\left(c_D,\left(1+\frac{\theta-1}{\Theta\gamma_E}\right)^{\frac{\alpha_D}{2}}\frac{(\Theta\gamma_E)^{\frac{\alpha_D}{2}}}{\beta_D}\right)d\gamma_E\right),
\end{aligned} \tag{4}$$

where $C_{th}(C_{th}\ge 0)$ is the target secrecy capacity threshold, and $\Theta=\exp(C_{th})\ge 1$, $\beta_k=\frac{(\bar{\gamma}_k)^{\alpha_k/2}}{c_k}(k\in\{D,E\})$.

Clearly, it is difficult to solve Eq. (4) because the integration involves complicated integral of polynomial power. But from Eq. (4), we can obtain

$$\Upsilon\left(c_D,\left(1+\frac{\Theta-1}{\Theta\gamma_E}\right)^{\frac{\alpha_D}{2}}\frac{(\Theta\gamma_E)^{\frac{\alpha_D}{2}}}{\beta_D}\right)\underset{=}{\gamma_E\to\infty}\Upsilon\left(c_D,\frac{(\Theta\gamma_E)^{\frac{\alpha_D}{2}}}{\beta_D}\right). \tag{5}$$

Thus, instead of seeking the exact closed-form expression for SOP, we derive the lower bound of SOP by adopting a similar method proposed in [4] as

$$SOP=P\{\gamma_D\le\Theta\gamma_E+\Theta-1\}\ge SOP^L=P\{\gamma_D\le\Theta\gamma_E\}. \tag{6}$$

Using Eqs. (2) and (3), we can obtain the lower bound of SOP as

$$\begin{aligned}
SOP^L &= P\{\gamma_D<\Theta\gamma_E\}\\
&= \frac{\alpha_E}{2\beta_E^{c_E}\Gamma(c_D)\Gamma(c_E)}\left(\int_0^\infty \gamma_E^{\frac{\alpha_E c_E}{2}-1}\right.\\
&\quad\times\exp\left(-\frac{\gamma_E^{\frac{\alpha_E}{2}}}{\beta_E}\right)\Upsilon\left(c_D,\frac{\Theta^{\frac{\alpha_D}{2}}\gamma_E^{\frac{\alpha_D}{2}}}{\beta_D}\right)d\gamma_E\\
&= \frac{1}{{\beta_E}^{c_E}\Gamma(c_D)\Gamma(c_E)}\int_0^\infty y^{c_E-1}\\
&\quad\times\exp\left(-\frac{y}{\beta_E}\right)\Upsilon\left(c_D,\frac{\Theta^{\frac{\alpha_D}{2}}y^{\frac{a}{b}}}{\beta_D}\right)dy,
\end{aligned} \tag{7}$$

where $y=\gamma_E^{\alpha_E/2}$, $\frac{a}{b}=\frac{\alpha_D}{\alpha_E}$, a and b are positive integers mutually prime numbers.

In the following, we will use two methods to calculate the integral in Eq. (7).

A. Methods I

As suggested by. Eq. (11) in [21], Eqs. (7.11.3/1) and (8.4.51/1) in [22], the logarithmic and lower incomplete Gamma function in Eq. (7) can be rewritten in the form of Meijer's G-function [19, eq. (9.301)] as

$$\exp\left(-\frac{y}{\beta_E}\right)=G_{0,1}^{1,0}\left[\frac{y}{\beta_E}\big|_0^-\right], \tag{8}$$

$$\begin{aligned}
\Upsilon\left(c_D,\frac{\Theta^{\frac{\alpha_D}{2}}y^{\frac{a}{b}}}{\beta_D}\right) &= \frac{\Gamma(c_D+1)}{\Gamma(c_D)c_D}\left(\frac{\Theta^{\frac{\alpha_D}{2}}y^{\frac{a}{b}}}{\beta_D}\right)^{c_D}\\
&\quad\times G_{1,2}^{1,1}\left[\frac{\Theta^{\frac{\alpha_D}{2}}y^{\frac{a}{b}}}{\beta_D}\big|_{0,-c_D}^{1-c_D}\right].
\end{aligned} \tag{9}$$

Then, substituting Eqs. (8) and (9) into Eq. (7), and using Eq. (21) in [21], the integral in Eq. (7) can be solved in closed-form and the lower bound of SOP can be obtained by Eq. (10), shown at the bottom of the next page, where $\Delta(k,a)=\frac{a}{k},\frac{a+1}{k},\ldots,\frac{a+k-1}{k}$.

B. Methods II

Using Eq. (3.10.1/8) in [23], the lower bound of SOP can be obtained by Eq. (11), shown at the bottom of the next page.

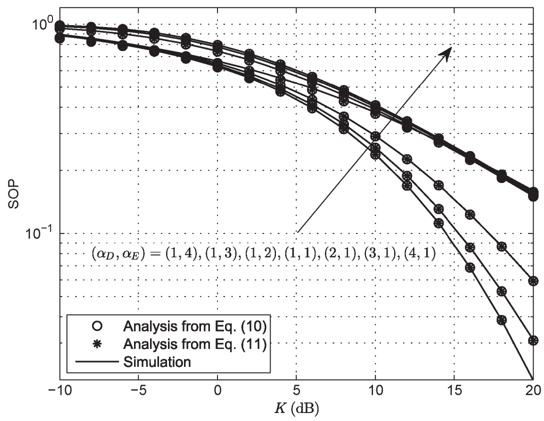

Fig. 1. SOP for generalized Gamma channels versus K.

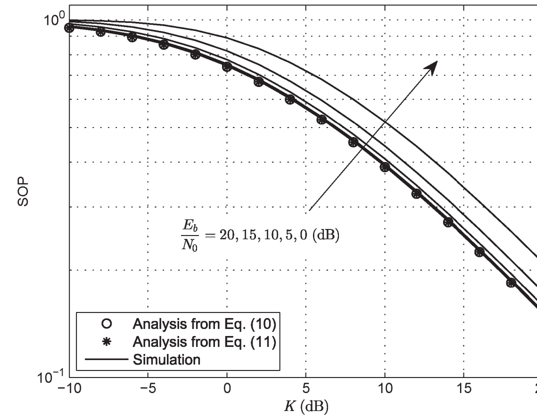

Fig. 2. SOP over generalized Gamma channels versus K.

IV. SPSC Analysis

The probability of SPSC, which is a fundamental benchmark in secure communications, can be obtained by

$$\begin{aligned} SPSC =& P\{C_s(\gamma_D, \gamma_E) > 0\} \\ =& 1 - \frac{\alpha_E}{2\beta_E^{c_E}\Gamma(c_D)\Gamma(c_E)} \left(\int_0^\infty \gamma_E^{\frac{\alpha_E c_E}{2} - 1} \right. \\ & \left. \times \exp\left(-\frac{\gamma_E^{\frac{\alpha_E}{2}}}{\beta_E} \right) \Upsilon\left(c_D, \frac{\gamma_E^{\frac{\alpha_D}{2}}}{\beta_D} \right) d_{\gamma E} \right). \end{aligned} \quad (12)$$

Similar to the derivation of Eqs. (10) and (11), one can solve Eq. (12) and obtain SPSC by Eqs. (13) and (14), shown at the bottom of the page.

One interesting finding can be found from Eqs. (10)–(14) that both the bound of SOP and SPSC do not change with $\frac{E_b}{N_0}$, although their expressions are the functions of $\frac{{\beta_E}^a}{{\beta_D}^b}$. It is because that, as $\frac{a}{b} = \frac{\alpha_D}{\alpha_E}$, $\beta_k = \frac{(\bar{\gamma}_k)^{\alpha_k/2}}{c_k} (k \in \{D, E\})$, we can have

$$\frac{{\beta_E}^a}{{\beta_D}^b} = \frac{{c_D}^b}{{c_E}^a} \left(\frac{\bar{r}_E^2 c_E^{-\frac{2}{\alpha_E}} \Gamma(c_D) \Gamma\left(C_E + \frac{2}{\alpha_E} \right)}{\bar{r}_D^2 c_D^{-\frac{2}{\alpha_D}} \Gamma(c_E) \Gamma\left(c_D + \frac{2}{\alpha_D} \right)} \right)^{b\alpha_D/2}. \quad (15)$$

Thus, it is clear that $\frac{{\beta_E}^a}{{\beta_D}^b}$ has no relationship with $\frac{E_b}{N_0}$.

V. Numerical Results and Discussions

In this section, numerical results and Monte-carlo simulations are presented to validate our analysis. The main parameters used in simulations and analysis are set as $C_{th} =$ 1 dB, $\bar{\gamma}_D = K\bar{\gamma}_E$ and $c_D = c_E = 1$. We plot the curves for various α_D and α_E for comparison purposes while K varying.

$$SOP_1^L = \frac{\Gamma(1+c_D)\Theta^{\frac{\alpha_D c_D}{2}} a^{\frac{a}{b}c_D + c_E - 0.5} b^{-0.5}}{C_D \left({\beta_D}^b / {\beta_E}^a \right)^{\frac{c_D}{b}} \Gamma(c_E)(2\pi)^{0.5(a+b)-1}} G_{b+a,2b}^{b,b+a} \left[\frac{\Theta^{\frac{b\alpha_D}{2}} a^a {\beta_E}^a}{b^b {\beta_D}^b} \middle| \begin{matrix} \Delta(b,1-c_D), \Delta\left(a, 1-\frac{a}{b}c_D - c_E\right) \\ \Delta(b,0), \Delta(b,-c_D) \end{matrix} \right] \quad (10)$$

$$SOP_2^L = \frac{b^{c_D - 0.5} a^{c_E - 0.5}}{\Gamma(c_E)\Gamma(c_D)(2\pi)^{0.5(a+b)-1}} G_{a+1,b+1}^{b,1+a} \left[\frac{\Theta^{\frac{b\alpha_D}{2}} a^a {\beta_E}^a}{b^b {\beta_D}^b} \middle| \begin{matrix} \Delta(a,1-c_E), 1 \\ \Delta(b,c_D), 0 \end{matrix} \right] \quad (11)$$

$$SPSC_1 = 1 - \frac{\Gamma(c_D+1) a^{\frac{a}{b}c_D + c_E - 0.5} b^{-0.5}}{C_D \left({\beta_D}^b / {\beta_E}^a \right)^{\frac{c_D}{b}} \Gamma(c_E)(2\pi)^{0.5(a+b)-1}} G_{b+a,2b}^{b,b+a} \left[\frac{a^a {\beta_E}^a}{b^b {\beta_D}^b} \middle| \begin{matrix} \Delta(b,1-c_D), \Delta\left(a, 1-\frac{a}{b}c_D - c_E\right) \\ \Delta(b,0), \Delta(b,-c_D) \end{matrix} \right] \quad (13)$$

$$SPSC_2 = 1 - \frac{b^{c_D - 0.5} a^{c_E - 0.5}}{\Gamma(c_E)\Gamma(c_D)(2\pi)^{\frac{b+a}{2}-1}} G_{a+1,b+1}^{b,1+a} \left[\frac{a^a {\beta_E}^a}{b^b {\beta_D}^b} \middle| \begin{matrix} \Delta(a,1-c_E), 1 \\ \Delta(b,c_D), 0 \end{matrix} \right] \quad (14)$$

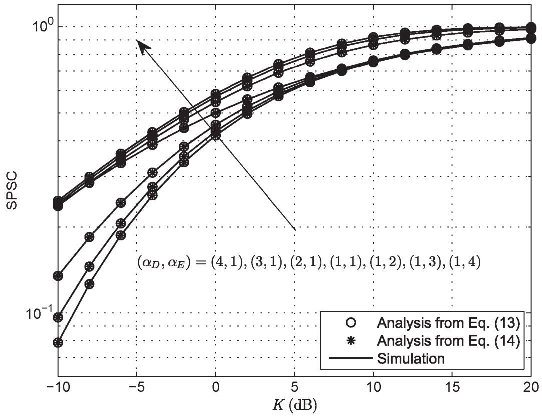

Fig. 3. SPSC over generalized Gamma channels versus K.

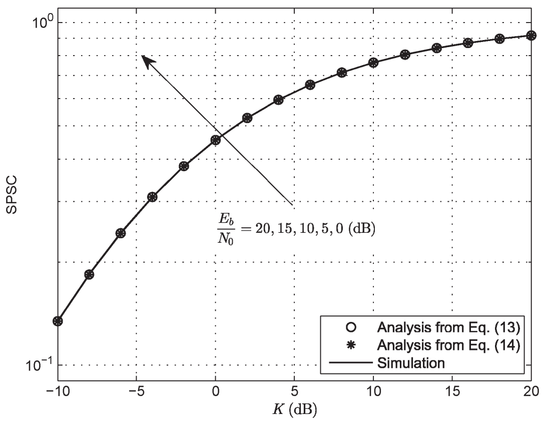

Fig. 4. SPSC over generalized Gamma channels versus K.

In Figs. 1–4, we compare simulation and analytical results of SOP and SPSC over GG fading channels. It is clear that analysis results match very well with simulation curves in Figs. 1, 3 and 4. Further, it can be observed that the SOP and SPSC for a higher K outperform than the ones for a lower K because a higher K represents that the main channel is better than the eavesdropper channel.

We can also find from Fig. 1 that SOP degrades while α_D increasing and α_E decreasing, which are the fading factors of the main and eavesdropper channels, respectively. From Fig. 2, one can observe that the simulated values gradually approach the analytical solutions as $\frac{E_b}{N_0}$ increases, which can be easily explained by Eq. (5). From Fig. 3, we obtain that SPSC can be improved while α_D decreasing and α_E increasing, since α_D and α_E represent the fading over the main and eavesdropper channels, respectively.

Moreover, from Figs. 2 and 4, we can see that the bound of SOP and the SPSC cannot be improved by increasing $\frac{E_b}{N_0}$. This observation agrees well with the finding from Eqs. (10)–(14) as shown in Section IV, which can be easily explained by Eq. (15).

VI. Conclusion

In this letter, we analyze the physical layer security for the classic Wyner's model over independent generalized Gamma Fading channels. The closed-form expressions for the probability of strictly positive secrecy capacity and the lower bound of secrecy outage probability have been derived and validated through simulations.

References

[1] X. Liu, "Strictly positive secrecy capacity of log-normal fading channel with multiple eavesdroppers," in *Proc. IEEE ICC*, Sydney, NSW, Australia, Jun. 2014, pp. 775–779.

[2] X. Liu, "Secrecy capacity of wireless links subject to log-normal fading," in *Proc. CHINACOM*, Kunming, China, Aug. 2012, pp. 167–172.

[3] X. Liu, "Probability of strictly positive secrecy capacity of the rician-rician fading channel," *IEEE Wireless Commun. Lett.*, vol. 2, no. 1, pp. 50–53, Feb. 2013.

[4] X. Liu, "Probability of strictly positive secrecy capacity of the weibull fading channel," in *Proc. IEEE GLOBECOM*, Atlanta, GA, USA, Dec. 2013, pp. 659–664.

[5] X. Liu, "Outage probability of secrecy capacity over correlated log-normal fading channels," *IEEE Commun. Lett.*, vol. 17, no. 2, pp. 289–292, Feb. 2013.

[6] X. Sun, J. Wang, W. Xu, and C. Zhao, "Performance of secure communications over correlated fading channels," *IEEE Signal Process. Lett.*, vol. 19, no. 8, pp. 479–482, Aug. 2012.

[7] Y. Zou, J. Zhu, X. Wang, and V. Leung, "Improving physical-layer security in wireless communications using diversity techniques," *IEEE Netw.*, vol. 29, no. 1, pp. 42–48, Jan. 2015.

[8] Y. Zou, X. Wang, and W. Shen, "Optimal relay selection for physical-layer security in cooperative wireless networks," *IEEE J. Sel. Areas Commun.*, vol. 31, no. 10, pp. 2099–2111, Oct. 2013.

[9] Y. Zou, B. Champagne, W. P. Zhu, and L. Hanzo, "Relay-selection improves the security-reliability trade-off in cognitive radio systems," *IEEE Trans. Commun.*, vol. 63, no. 1, pp. 215–228, Jan. 2015.

[10] E. W. Stacy, "A generalization of the gamma distribution," *Ann. Math. Statist.*, pp. 1187–1192, Jul. 1962.

[11] M. D. Yacoub, "The α-μ distribution: A general fading distribution," in *Proc. PIMRC*, Lisbon, Portugal, Sep. 2002, pp. 629–633.

[12] M. D. Yacoub, "The α-μ distribution: A physical fading model for the stacy distribution," *IEEE Trans. Veh. Technol.*, vol. 56, no. 1, pp. 27–34, Jan. 2007.

[13] G. Pan *et al.*, "Physical layer security over non-small scale fading channels," *IEEE Trans. Veh. Technol.*, DOI: 10.1109/TVT.2015.2412140, to be published.

[14] O. Gazi, "Bounds for generalized gamma distributed fading channels," *IEEE Commun. Lett.*, vol. 15, no. 12, pp. 1347–1349, Dec. 2011.

[15] V. A. Aalo, T. Piboongungon, and C. D. Iskander, "Bit-error rate of binary digital modulation schemes in generalized gamma fading channels," *IEEE Commun. Lett.*, vol. 9, no. 2, pp. 139–141, Feb. 2005.

[16] M. Hanif, H. Yang, and M. Alouini, "Capacity bounds for *k*th best path selection over generalized fading channels," *IEEE Commun. Lett.*, vol. 18, no. 2, pp. 261–264, Feb. 2014.

[17] A. D. Wyner, "The wire-tap channel," *Bell Syst. Tech. J.*, vol. 54, no. 8, pp. 1355–1387, Oct. 1975.

[18] P. M. Shankar, *Fading and Shadowing in Wireless Systems*. New York, NY, USA: Springer Science Business Media, 2012.

[19] I. Gradshteyn and I. Ryzhik, *Table of Integrals, Series and Products*, 7th ed. San Diego, CA, USA: Academic, 2007.

[20] M. Bloch, J. Barros, M. R. Rodrigues, and S. W. McLaughlin, "Wireless information-theoretic security," *IEEE Trans. Inf. Theory*, vol. 54, no. 6, pp. 2515–2534, Jun. 2008.

[21] V. S. Adamchik and O. I. Marichev, "The algorithm for calculating integrals of hypergeometric type functions and its realization in REDUCE system," in *Proc. ISSAC*, New York, NY, USA, 1990, pp. 212–224.

[22] A. P. Prudnikov, Y. A. Brychkov, and O. I. Marichev, *Integrals and Series: Vol. 3: More Special Functions*. New York, NY, USA: CRC Press, 1992.

[23] A. P. Prudnikov, Y. A. Brychkov, and O. I. Marichev, *Integrals and Series: Vol. 4: Direct Laplace Transforms*. New York, NY, USA: CRC Press, 1992.